Dielectric properties of silver borophosphate glasses

R. A. HASHMI, NOOR-UL HAQUE, N. BANO, M. K. ANIS
Condensed Matter Research Laboratory, Department of Physics, University of Karachi, Karachi 75270, Pakistan

Dynamic behaviour of electrical conduction and polarization in silver borophosphate glasses has been studied over wide range of frequencies and temperatures. The dielectric spectrum showed a strong dispersion in $C'(\omega)$ with rise in temperature which distinguishes the conduction process from a pure steady state. The observed behaviour was found to be temperature activated with an activation energy of 0.39 eV. The data have been analysed in terms of admittance plots and a model has been proposed on the basis of this analysis.

1. Introduction
Glasses are an inorganic product of fusion which has been cooled to rigid condition without crystallization [1]. Inorganic materials, such as silica, sand, sodium, calcium, carbonates feldspars, borate and phosphate, are used to make glasses [2]. The large variation in composition coupled with lack of long-range structure has created interest in these materials not only from technologists as potential materials for solid state ionic devices, but also from physicists because of their intricate conduction mechanisms that are being proposed to explain the unusually high ionic conductivity in some of the recently studied amorphous solid electrolyte systems [2–10].

In most oxide glasses, the electrical conductivity results from ionic motion. D.c. and a.c. measuring techniques have been used to study the electrical properties of these materials. In d.c. measurements, a space-charge region is often set up because of the partial blocking of the ionic current by the electrodes which causes the current to fall rapidly with time. This problem can be eliminated by using a.c. impedance spectroscopy [8, 11, 12]. The use of a.c technique, not only eliminates the problems associated with d.c measurements, but it permits the determination of ionic conductivity and relaxation time [12]. Studies of complex impedance and complex modulus formalisms require the measurement of dielectric parameters (C' and C'' or ε' and ε'') over a wide range of frequencies. Dielectric studies of solids and liquids have been the subject of intense continuing investigation over a long period of time. A detailed survey of the dielectric properties of a wide range of solids has been given by Jonscher [13–15]. It was observed that the dielectric response of solids departs significantly from the ideal Debye response and can be expressed in terms of fractional power laws, according to which the frequency dependence of the complex capacitance of all solids in which the dielectric behaviour is dominated by hopping charge carriers, is given by

$$\tilde{C}(\omega) = A(i\omega)^{(n_1-1)} + B(i\omega)^{(n_2-1)} \tag{1}$$

where A and B are suitable constants and the exponents n_1 and n_2 lie between zero and 1. n_1 dominates at high frequencies falling closer to unity, whereas n_2 dominates at low frequencies and is close to zero. The low-frequency behaviour corresponding to $n_2 = 0$ is referred to as low-frequency dispersion (LFD) [16–18].

An essential feature of Equation 1 is that the ratio of the real and imaginary components of the complex capacitance is frequency independent, in complete contrast with the classical Debye relation

$$C''(\omega)/C'(\omega) = \cot(n\pi/2) \tag{2}$$

In this paper we report the dielectric properties of silver borophosphate glasses ($Ag_2O:B_2O_3:P_2O_5$) of composition 60:08:32 over a wide range of frequencies and temperatures. The experimental data confirms the presence of the power law [1].

2. Experimental procedure
The chemicals used for the preparation of glasses of different compositions were reagent-grade $AgNO_3$ (JM), P_2O_5 (Merck) and B_2O_3 (BDH). A mixture of these compounds in the desired stoichiometric ratio by weight, was taken in a platinum crucible. After thorough mixing, it was heated in a muffle furnace between 900 and 1100 °C for about 30 min. The glass pellets, 12 mm diameter and 2.4 mm thick, were prepared by a conventional air-quenching technique in a specially designed steel die.

X-ray diffraction analysis confirmed that the prepared silver borophosphate glass samples have amorphous structure. The pellets were smoothed and then cleaned in an ultrasonic bath. Gold contacts ($\approx$ 1 µm thick and 0.86 cm diameter) were deposited on both sides of the pellets at residual pressure, $\sim 10^{-5}$ torr (1 torr = 133.322 Pa). For electrical connection, fine copper wires were connected to the gold electrodes of the sample using silver conducting paint.

The sample was mounted with a heat-sinking compound on the copper base of the sample holder of the Oxford 1704 cryostat. The sample temperature was controlled and maintained by ITC4 (Oxford).

Frequency domain measurements, at different temperatures under vacuum ($\approx 10^{-3}$ torr) were carried out using a Solartron frequency response analyser (FRA) 1255 in conjunction with a Chelsea Dielectric interface coupled to Opus PC. The results were plotted through Roland DXY-880A X-Y plotter in the form of real ($C'(\omega)$) and imaginary (G/ω) components of the complex capacitance, conductance $G(\omega)$ and $\tan\delta$ as a function of the circular frequency $f = \omega/2\pi$ in logarithmic coordinates. The print out of numerical data was taken with an Epson LQ500 printer and stored on floppy disk for further processing. All the samples were studied at 0.1 V r.m.s and with 0 V d.c. bias in the frequency range 10^{-4}–10^5 Hz and temperature range 120–400 K.

3. Results and discussion

The frequency dependence of both the real, $C'(\omega)$, and imaginary components, $C''(\omega)$, of the complex capacitance for silver borophosphate glass

(Ag_2O:B_2O_3:P_2O_5, 60:08:32) is shown in Fig. 1a and b for high and low temperatures, respectively. Both $C'(\omega)$ and $C''(\omega)$ are plotted on a log–log scale on common axes and the individual sets are displaced vertically by two decades for clarity of presentation. It is evident from these figures that the dielectric response of the sample is a strong function of temperature, both qualitatively and quantitatively. At the lowest temperature (120k) the $C'(\omega)$ remains practically flat over the whole measured frequency range. The scattering in $C''(\omega)$ in the intermediate frequency range is due to very low values of conductance.

A clear dispersion in $C'(\omega)$ is observed with rise in temperature and three different regions, namely, a constant $C'(\omega)$ at high frequencies followed by a rapid rise at intermediate frequencies, and finally a tendency towards saturation at lower frequencies can clearly be identified in the spectrum. The frequency range for each region is shifted towards high frequencies with the rise in sample temperature. Thus the constant $C'(\omega)$ behaviour observed below room temperature almost disappears at higher temperatures.

Below 275 K, the value of $C'(\omega)$ at higher frequencies is almost independent of temperature, which may be correlated to the geometrical capacitance of the
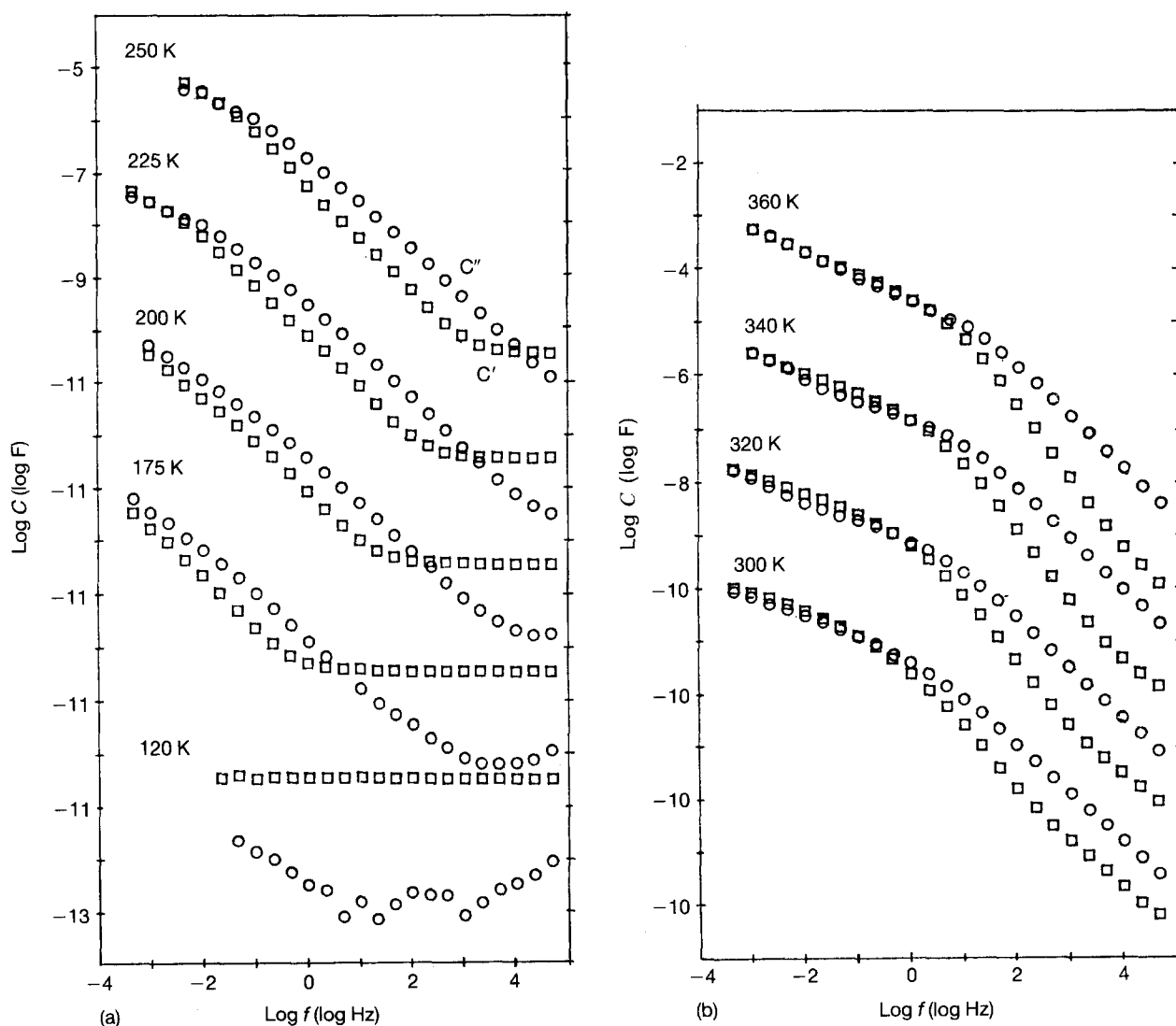

Figure 1 The frequency dependence of ($\square$) $C'(\omega)$ and ($\bigcirc$) $C''(\omega)$ of a silver borophosphate glass sample, (a) below room temperature, and (b) above room temperature. The consecutive sets corresponding to rising temperature are displaced vertically by two decades for clarity.

sample. The slopes of the $C'(\omega)$ curves depend significantly on temperature, and increase with rise in temperature. This implies that the process responsible for the observed rise in $C'(\omega)$ is temperature-activated.

The third region of the spectrum corresponding to the lower frequencies shows a relatively slow rise in $C'(\omega)$. The flattening of the spectrum at lower frequencies is understandable, as the behaviour is temperature-dependent and shifts towards higher frequencies with the increase in temperature. Hence, the frequency range corresponding to this behaviour is under the measuring window of our instrument at higher temperatures, whereas, at low temperatures the frequency is below the lower limit of our measurements (10^{-3} Hz). Although the flat region shifts towards higher frequencies with the increase in temperature, the corresponding slopes (0.35–0.46) show a small variation with temperature (300–360 K). This implies that the mechanism responsible for this behaviour is weakly temperature dependent.

The $C''(\omega)$ curves also give two different slopes for different frequency range. At higher frequencies (above 1 Hz) the slopes are very steep, whereas below 1 Hz, the increase in $C''(\omega)$ with frequency is significantly slow and the curves for $C'(\omega)$ and $C''(\omega)$ almost coincide with each other.

The steep rise in $C''(\omega)$ at higher frequencies is weakly temperature-dependent. Below room temperature the slopes have same values (0.87), which are significantly different from unity. Above room temperature the corresponding slopes show increase with temperature but still remain less than one. It may be noted here that a unity slope of $C''(\omega)$ versus frequency curve corresponds to a pure steady-state conduction, which is not observed in our samples. The increase in slopes of $C''(\omega)$ curves with temperature implies that the d. c. contribution increases with rise in temperature and this contribution is almost negligible below 200 K.

The total conductance is the sum of two components: a pure d. c. conductance, G_0, which is independent of frequency and a frequency-dependent conductance, $G(\omega)$

$$G(\omega) = G_0 + G(\omega) \qquad (3)$$

$$C''(\omega) = G/\omega = G_0/\omega + G(\omega)/\omega \qquad (4)$$

Both G_0 and $G(\omega)$ are temperature sensitive and hence the total conductance increases with rise in temperature, as shown in Fig. 2, where values of log G at two different frequencies are plotted against reciprocal of temperature. The resulting straight lines show a good Arrhenius plot with activation energy 0.39 eV.

Although a large dispersion in $C'(\omega)$ is observed at low frequencies, particularly at high temperatures, exact parallelism between $C'(\omega)$ and $C''(\omega)$ is not found as required by Equation 2. This lack of parallelism between the real and imaginary capacitance implies that the pure LFD process is perturbed by the presence of other processes which can be sorted out by transforming the data into the complex impedance or admittance plots [13, 18]. The choice between Y- and Z-plots as the correct representation depends upon
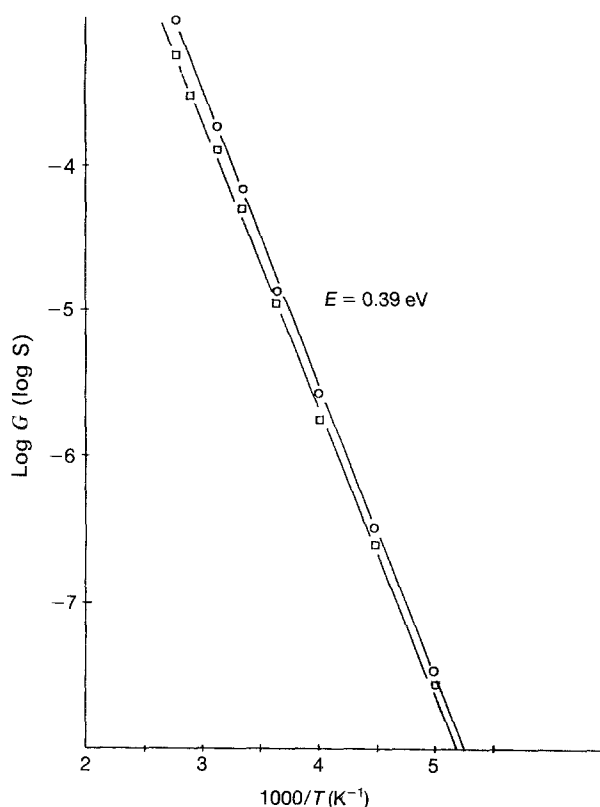

Figure 2 Variation of conductance at ($\square$) 10 Hz and ($\bigcirc$) 100 Hz with temperature. The resulting straight lines on a semi-logarithmic plot give activation energy $E = 0.39$ eV.

the nature of the particular response; for our data, Y-plots are found to be more suitable. Typical admittance plots for our samples at three different temperatures are shown in Fig. 3. It is evident from Fig. 3 that Y-plots consist of three elements which can be identified as follows:

(a) an almost vertical straight line (spike) at high frequencies which dominates the low temperature plots. With increase in temperature, the high-frequency component of Y-plots appears as a spur and finally it disappears at the highest temperature (360 K);

(b) at lower frequencies a skewed semi-circle is observed at all temperatures and the diameter of the circle increases with the rise in temperature;

(c) at intermediate frequencies the low-temperature data correspond to an almost flat element in the Y-plane.

In Y-representation, a vertical straight line corresponds to a loss-free (perfect) capacitor, and a skewed semi-circle represents a series combination of a dispersive capacitor, C_n, and an (imperfect) conductor, G.

In the light of these general features of admittance representation, the high-frequency spike observed at low temperatures represents the bulk conductance of the sample and the behaviour is similar to an almost loss-free capacitor. The conductance is a temperature-dependent parameter and with rise in temperature the ideal bulk response would shift towards much higher frequencies, which is beyond the frequency range of our measurements. Thus, in the high-temperature
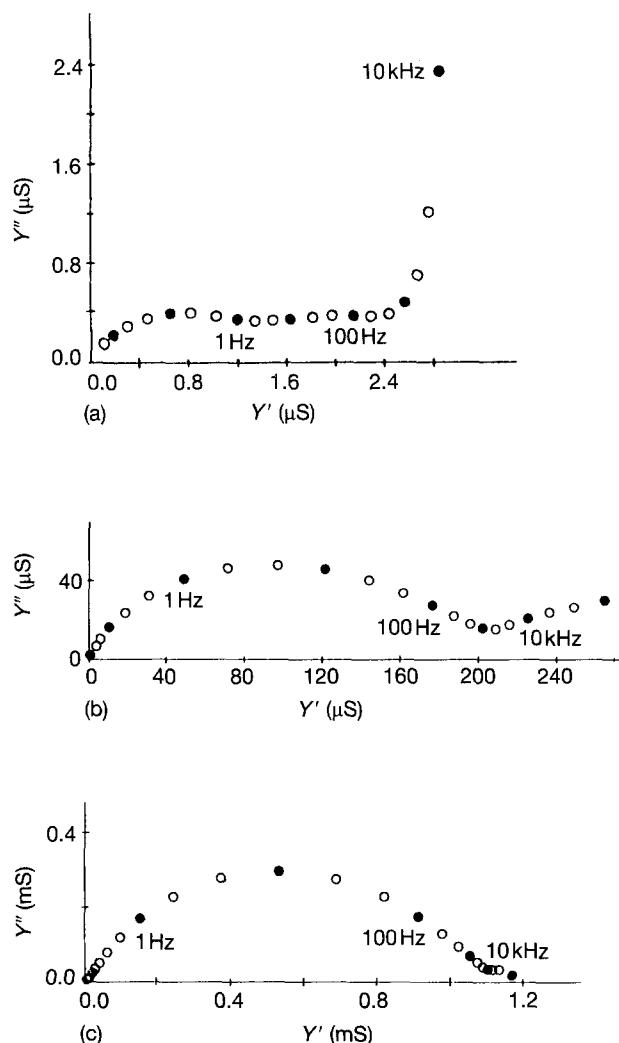
6613

Figure 3 The complex admittance plots at three selected temperatures. (a) 250 K, (b) 320 K, (c) 360 K.

Figure 4 Proposed equivalent circuit for the studied silver borophosphate glass samples.

data, no straight line element in admittance plots is observed.

At all temperatures the low-frequency data corresponds to a series combination of an imperfect capacitor, C_n, and an imperfect conductor, $G(\omega)$. n is the measure of dispersiveness of C_n, and is related to the angle of inclination of the circular arc to the real axis, and the diameter of the circular arc corresponds to the value of $G(\omega)$. For our samples, G is found to increase with rise in temperature whereas, both C_n and n are almost temperature independent. This suggests that the dispersive behaviour of C_n is intrinsic property of the sample and is independent of temperature. It may be possible that the glass–electrodes interface acts as blocking capacitor. With rise in temperature, ionic mobility will increase and will cause diffusion of these ions across the interface. The higher the temperature, the wider is the diffusion region. The diffusion process can also be noted from the capacitance plots (Fig. 1), where $C'(\omega)$ and $C''(\omega)$ curves coincide with each other.

The almost flat Y'' observed at low temperatures and intermediate frequencies represents a highly temperature dependent dispersive element; with rise in temperature it not only shifts to higher frequencies but also changes into an inclined spur.
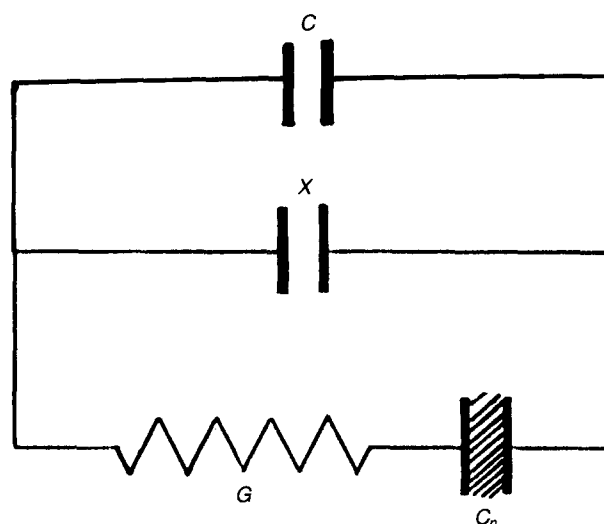
The above discussion suggests that the general response of our samples can be represented by parallel combination of three different components, as shown in Fig. 4. C is an almost loss-free capacitor, X is a temperature sensitive element, C_n is a dispersive capacitor with n ranging between 0.6 and 0.7, and G is an imperfect conductor. The value of G is very low at low temperatures and the total response is dominated by C. At high temperature, G is relatively large and the series combination of $G(\omega)$ and C_n becomes effective. In fact, temperature shifts the whole response towards higher frequencies and thus the effect of C is not observed at high temperature as it is out of the upper limit of our frequency range and the contribution of G and C_n (in series with each other) extends over the whole frequency range.

Acknowledgements

References

1. A. PAUL, "Chemistry of Glasses" (Chapman and Hall, London, New York, 1990) Ch. 1.
2. R. H. DOREMUS, "Glass Science", (Wiley, New York, 1973).
3. B. V. R. CHOWDARI and S. RADHAKRISHNA, (eds), "Proceedings of the Seminar on Solid State Ionic Devices" (World Scientific, Singapore, 1988).
4. Idem, "Proceedings of a Workshop on Materials for Solid State Batteries" (World Scientific, Singapore, 1986).
5. A. MAGISTRIS and G. CHIODELLI, Solid State Ionics 9, 10 (1983) 611.
6. G. CHIODELLI, C. VIGANÖ, G. FLOR, and A. MAGISTRIS, ibid. 8 (1983) 311.
7. B. V. R. CHOWDARI and S.K. AKHTER, J. Non-Cryst. Solids 116 (1990) 16.
8. I. M. HODGE, M. D. INGRAM and A. R. WEST, J. Electroanal. Chem. 74 (1976) 125.
9. H. L. TULLER, D. P. BUTTON, and D. R. UHLMANN, J. Non-Cryst. Solids 40 (1980) 93.
10. B. V. R. CHOWDARI, R. GOPALAKRISHNAN, S. H. GOH and K. L. TARI, J. Mater. Sci. 23 (1988) 1248.

11. R. J. GRANT, M. D. INGRAM, L. D. S. TURNER and C. A. VINCENT, *J. Phys. Chem.* **82** (1978) 2838.
12. J. R. MACDONALD, *J. Appl. Phys.* **58** (1985) 1956.
13. A. K. JONSCHER "Dielectric Relaxation in Solids." (Chelsea Dielectric Press, London, 1983).
14. *Idem. J. Mater. Sci.* **26** (1991) 1618.
15. *Idem*, in "Conference Proceedings Properties and Applications of Dielectric Materials", Tokyo (1991).
16. R. M. HILL and A. K. JONSCHER, *Contemp. Phys.* **24** (1983) 75.
17. L. A. DISSADO and R. M. HILL, *J. Chem. Soc. Farad. Trans.* 2 **80** (1984) 291.
18. N. BANO and A. K. JONSCHER *J. Mater. Sci.* **27** (1992) 1672.